Optical waveguide splitters based on multimode interference structures made by ion exchange in glass

MAREK BŁAHUT

Institute of Physics, Silesian University of Technology, ul. Bolesława Krzywoustego 2, 44—100 Gliwice, Poland.

In the paper, numerical studies of gradient index optical splitters made using a multimode interference technology are presented. Multimode interference structures produced in $K^+ \longleftrightarrow Na^+$ and $Ag^+ \longleftrightarrow Na^+$ ion exchange processes have been compared. The influence of geometrical parameters of multimode interference structure and technological process parameters is examined in numerical simulations. Based on the above, gradient index optical waveguide splitters and Mach –Zehnder interferometers in multimode interference configuration are proposed.

1. Introduction

Multimode interference (MMI) structures have been subjected to intensive theoretical and technological studies for the last few years [1]—[3]. It is a technology that makes use of modal fields interference effects in multimode waveguide forming a multimode interference section. Intermode interference (general or restricted [1]) is accompanide by so-called self-imaging phenomena of the input field exciting multimode waveguide. As a result of these effects, the input field coming from a single-mode waveguide or a group of single-mode waveguides is reproduced in simple, reflected and multiple images.

A large majority of works on MMI concerned interference structures made on the basis of step-index waveguides. In paper [4], the possibility of self-imaging effects appearing in gradient-index waveguides made by $K^+ \longleftrightarrow Na^+$ in glass substrate, which can be used in $1 \times N$ power splitters fabrication, is shown.

Gradient structures made by ion exchange in glass are particularly attractive for MMI technology. Owing to the ion exchange technique that makes use of multi-step diffusion processes, electrodiffusion, heating, diffusive and electrodiffusive burying it is possible to easily changes the modal properties of waveguides obtained on which the intermode interference effects rely.

In this work, the optimization studies of gradient MMI optical waveguide splitters in symmetrical configuration made in two basic processes of ion exchange $K^+ \longleftrightarrow Na^+$ and $Ag^+ \longleftrightarrow Na^+$ are presented. The influence of geometrical parameters of MMI structure and technological process parameters are examined in numerical simulations. Based on the above, gradient index optical waveguide splitters and Mach–Zehnder interferometers in MMI configuration are proposed.

2. Method of analysis

A diagram of the MMI structure examined is presented in Fig. 1. It consists of a monomode input waveguide obtained by the ion diffusion process through the window of the width w, symmetrically situated to a wide multimode section of the window width W_M and the length L, where we can observe the effects of interference of mode fields and a pair of monomode output waveguides of the input geometry. In that case only symmetric modes are excited. Output waveguides are situated at sites of the output signal maximum when double input field images appear.
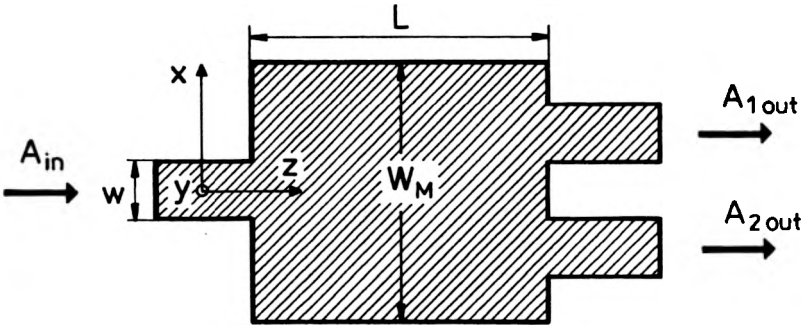

Fig. 1. Diagram of MMI structure under examination.

Wave propagation in the structure presented is analysed on the basis of scalar finite difference beam propagation method (FD BPM), [4]. The starting point of FD BPM is a scalar Helmholtz equation. Assuming TE polarization, we have in a three-dimensional case

$$\frac{\partial^2 E}{\partial x^2}+\frac{\partial^2 E}{\partial y^2}+\frac{\partial^2 E}{\partial z^2}+n^2(x,y,z)k^2 E(x,y,z)=0 \tag{1}$$

where $n(x,y,z)$ is the refractive index and $k=\omega/c$. A scalar field distribution $E(x,y,z)$ can be written according to the slowly varying envelope approximation as

$$E(x,y,z)=u(x,y,z)\exp(jkn_0) \tag{2}$$

where n_0 is a real reference constant (assuming $n_0=\beta_0/k$, where β_0 is the propagation constant of monomode waveguide), [5]. Substituting it into (1) yields in paraxial approximation [4]

$$-2jkn_0\frac{\partial u}{\partial z}=\frac{\partial^2 u}{\partial x^2}+\frac{\partial^2 u}{\partial y^2}+k^2(n^2-n_0^2)u. \tag{3}$$

Equation (3) is solved numerically using the alternating direction implicit method [6] and Cranck–Nicholson finite difference scheme with transparent boundary conditions [7] at the edge of computational window. The number of transverse grid points $N_x \times N_y$, grid dimensions Δx, Δy and the step of propagation Δz for both exchange processes are listed in Tab. 1. In each step of calculations, beginning

T a b l e 1. Numerical parameters of calculations.

	$K^+ \longleftrightarrow Na^+$	$Ag \longleftrightarrow Na^+$
Grid point $N_x \times N_y$	$400 \times 100^*$	$200 \times 50^{**}$
Grid dimension Δx, Δy [μm]	0.25	0.1
Propagation step Δz [μm]	0.5	0.25

* 500×100 for $W_M = 100$ μm.
** 400×50 for $W_M = 20$ and 25 μm.

with the initial field distribution at $z = 0$ μm, the field distribution at propagation step $z + \Delta z$ is expressed in terms of the field at propagation step z.

Input field (Gauss distribution) fits, after having passes a short path, to monomode field distribution and the stable field propagation of the amplitude equal A_{in} is observed. When the monomode field reaches the interference section input, it is decomposed to mode fields of the multimode waveguide.

Fields in output waveguides achieve after having passes a short path the wave function distributions of single-mode waveguide of the amplitudes A_{1out} and A_{2out}. Insertion loss α [dB] in power splitter, taking into consideration the input field imaging inaccuracy in interference section and coupling losses to output waveguides, is decribed by the equation

$$\alpha = -10 \log \frac{A^2_{1out} + A^2_{2out}}{A^2_{in}}. \tag{4}$$

3. Self-imaging processes in multimode gradient interference structures

The basic elements of MMI gradient sections investigated are multimode waveguides made by $K^+ \longleftrightarrow Na^+$ and $Ag^+ \longleftrightarrow Na^+$ ion exchange method, whose two-dimensional refractive index distribution profiles are numerically calculated from the nonlinear diffusion equation [8]. The substrate is borosilicate glass of the refractive index 1.51 situated at $y = 3$ μm and surrounded by air. Material parameters of the ion exchange used in our calculation, determined on the basis of IWKB method, are listed in Tab. 2.

T a b l e 2. Material parameters of ion exchange processes.

	$K^+ \longleftrightarrow Na^+$	$Ag^+ \longleftrightarrow Na^+$
Diffusion depth $(Dt)^{1/2}$ [μm²/h]	1.269	0.31
Mobility ratio r	0.9	0.5
Maximum index change Δn	0.0084	0.1

The geometry and technological process parameters are selected in such a way that in all analyzed cases the interference section is multimode for the direction consistent with the structure width (x-direction) and single-mode for the perpen-

dicular direction y, and thus, only one-dimensional interference effects occur during the light propagation.

The dependences of propagation constants on the mode number of multimode sections, similarly to the step-index structures, are nearly quadratic and self-imaging phenomena related to general and restricted − paired and symmetric − interference can be observed [1].
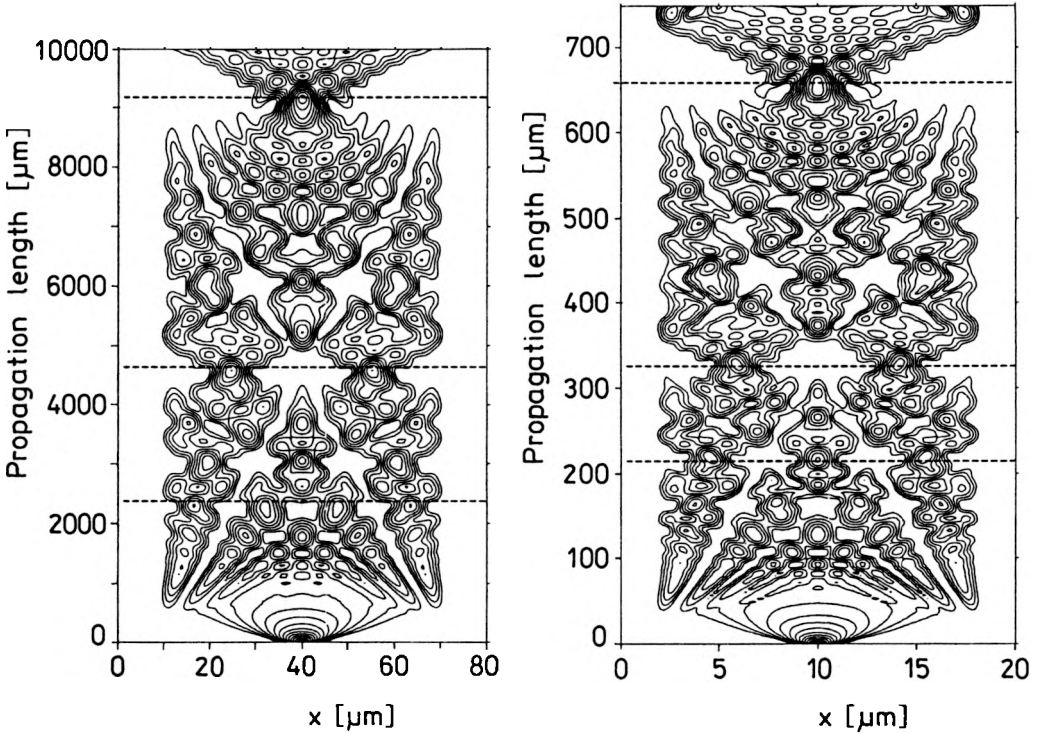
Fig. 2. Contour map distributions of the amplitude along propagation path for $K^+ \longleftrightarrow Na^+$ ion exchange MMI structure. The minimal amplitude contour is equal to 0.25 of the maximum value.

Fig. 3. Contour map distributions of the amplitude along propagation path for $Ag^+ \longleftrightarrow Na^+$ ion exchange MMI structure. The minimal amplitude contour is equal to 0.25 of the maximum value.

Figures 2 and 3 present contour map distributions of the amplitude $A(x, y_{max})$ (y_{max} corresponds to the maximum of distribution) along propagation path for the structure MMI excited symmetrically with the field of single-mode waveguide of the wavelength of $\lambda = 0.6328$ μm, obtained by $K^+ \longleftrightarrow Na^+$ ion exchange (single-mode waveguide window $w = 5$ μm and multimode section window width $W_M = 60$ μm) and $Ag^+ \longleftrightarrow Na^+$ ($w = 1.2$ μm, $W_M = 16$ μm) for the minimum reference level 0.25 of maximum value. Both multimode interference sections guide, for comparison, modes of the same mode number 12 for the process parameters and geometry chosen.

Comparing interference distributions, it can be noticed that, for the sake of large refractive index change difference (over 10 times greater for $Ag^+ \longleftrightarrow Na^+$ ion

exchange), input field images are formed for this exchange at the coupling lengths of 658 μm, considerably shorter in comparison to the coupling length of 9190 μm for $K^+ \longleftrightarrow Na^+$ ion exchange and are localized over a smaller area. This is the result of substantial differences of zero and first order propagation constants of the analyzed structures. However, despite of scale difference, both distributions are very similar. At the distances L/n symmetrical n-fold images of input field are observed. Propagation sections for $n = 4, 2, 1$ are marked in Figs. 2, 3.

The results obtained show the possibility of applying gradient MMI structures as optical waveguide splitters where the input field division proceeds over the small area of several-hundred micrometers. However, it can be seen that the observed interference images reproduce the input field only approximately. The quality of interference images gets worse also with an increase of propagation length.

4. Optical waveguide splitters 1×2

Working characteristics of optical waveguide splitters depend on structure geometry and technological process parameters. The present study concerns the influence of the input waveguide and MMI section window width and effect of the heating of single-mode waveguide and multimode section refractive index profiles. Table 2 describes technological process parameters used in calculations.

4.1. Influence of input waveguide width

The input waveguide window width was changed for the fixed width of MMI sections ($W_M = 40$ μm for $K^+ \longleftrightarrow Na^+$ ion exchange and $W_M = 16$ μm for $Ag^+ \longleftrightarrow Na^+$) symmetrically excited. The interference path corresponds to the coupling length $L_{3\,dB}$ for twofold images. Insertion losses in optical waveguide splitter were determined from Eq. (2). Results of numerical simulations are shown in Tables 3 and 4.

T a b l e 3. Insertion losses for different input waveguide window widths for $K^+ \longleftrightarrow Na^+$ ion exchange.

w [μm]	Loss α [dB]
2	5.257
3	0.903
4	0.656
5	0.520

T a b l e 4. Insertion losses for different input waveguide window widths for $Ag^+ \longleftrightarrow Na^+$ ion exchange.

w [μm]	Loss α [dB]
0.6	1.443
0.8	1.249
1.0	0.881
1.2	0.709

The single-mode waveguide window for $K^+ \longleftrightarrow Na^+$ ion exchange was changed in the range of $2-5$ μm (for the window width above 5.6 μm the waveguide becomes two-mode). The coupling length L_{3dB}, connected with MMI section width, was 2120 μm.

The window width for $Ag^+ \longleftrightarrow Na^+$ exchange varied in the range of $0.6-1.2$ μm (above 1.3 μm the waveguide becomes two-mode). The coupling length L_{3dB} amounted to 319 μm in all the cases investigated.

As shown by the calculation results for both ion exchange processes, an increase of the window width causes a decrease in insertion losses at the output of the splitter. Exceptionally large insertion loss for the narrow window of the width of 2 μm ($K^+ \longleftrightarrow Na^+$ ion exchange) results from the single-mode field propagation close to the cut-off point of the basic mode and fields overlap at the splitter output, as shown in Figs. 4 and 5.
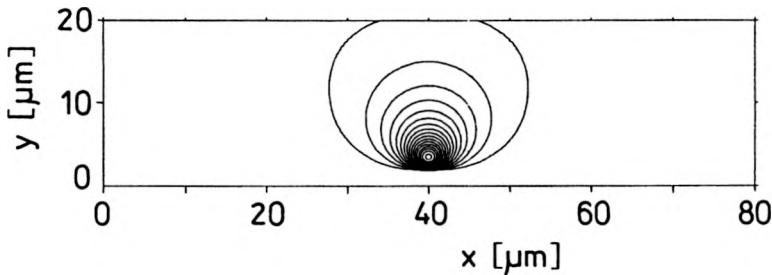

Fig. 4. Contour map of the input field distribution for $K^+ \longleftrightarrow Na^+$ ion exchange waveguide; $w = 2$ μm.
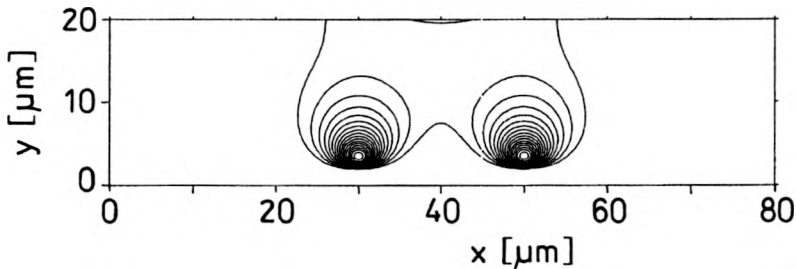

Fig. 5. Contour map of the out-put field distribution for $K^+ \longleftrightarrow Na^+$ ion exchange structure; $w = 2$ μm.

Summing up, the window width of single-mode input and output waveguides should be as big as to ensure good guiding conditions, which at its best are near the cut-off point of the first mode of higher order.

4.2. Influence of interference section width

The width of the MMI section window is of great importance for the working characteristics of the splitter. With an increase of MMI section width the number of guided modes also increases. This should make possible a precise and more detailed input field imaging. However, a greater window width means, at the sme time, lower

difference between propagation constants of zero and first order and thus, an increase of L_{3dB} coupling length [4]. Effects connected with the mismatch between the propagation constants β dependence on the mode number N and quadratic function can appear with increasing mode number. The increase of MMI section width with the width of monomode waveguide remaining constant can also lead to a larger geometrical mismatch of modal fields and larger insertion losses [3].

T a b l e 5. Insertion losses for different window widths of MMI structures for $K^+ \longleftrightarrow Na^+$ ion exchange.

Mode number	Window width [μm]	L_{3dB} [μm]	Loss α [dB]
7	40	2120	0.520
12	60	4595	0.681
17	80	7950	0.798
21	100	12300	0.884

T a b l e 6. Insertion losses for different window widths of MMI structures for $Ag^+ \longleftrightarrow Na^+$ ion exchange.

Mode number	Window width [μm]	L_{3dB} [μm]	Loss α [dB]
6	8	90.5	0.533
9	12	192	0.647
12	16	329	0.709
15	20	509	1.060
18	25	728	1.599

Results of numerical simulations are shown in Tables 5 and 6. The window width of MMI for $K^+ \longleftrightarrow Na^+$ ion exchange, centrally excited with the field of monomode waveguide of the window width 5 μm, was changed in the range of $40-100$ μm. It corresponds to a guided mode number of $7-21$. Calculations for $Ag^+ \longleftrightarrow Na^+$ ion exchange are carried out for MMI structures guiding a similar mode number $(6-18)$, for window widths within the range of $8-25$ μm, excited by the monomode field of the waveguide of 1.2 μm window width. Insertion losses increase along with MMI structure width in both cases. This demonstrates the superiority of the effects connected with geometrical mismatch and deviation of $\beta(N)$ dependence on quadratic relation. It should also be noted that MMI sections of both exchange processes guiding a similar mode number show comparable insertion losses.

Optimum widths of MMI section equal to 40 μm for $K^+ \longleftrightarrow Na^+$ ion exchange and 8 μm for $Ag^+ \longleftrightarrow Na^+$ ensure output fields separation and low insertion losses. Field distribution evolutions propagating through splitters described are shown in Figs. 6 and 7.

4.3. Influence of the time of heating

The heating of refractive index profiles obtained in preliminary diffusion is one of the ways of modifying mode characteristics. Reducing the maximum refractive index change and widening the distribution profile changes modal field distribution of in-
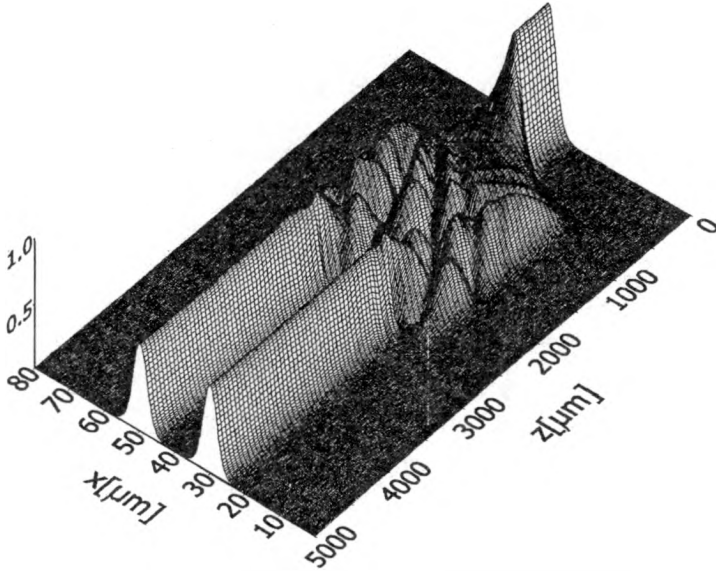
Fig. 6. Distribution of field amplitude in $K^+ \longleftrightarrow Na^+$ ion exchange waveguide splitter 1×2; $W_M = 40$ µm, $w = 5$ µm.
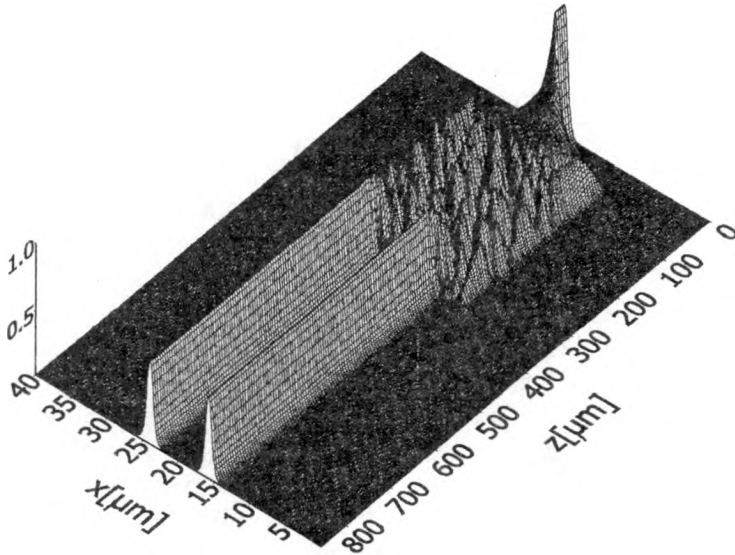

Fig. 7. Distribution of field amplitude in $Ag^+ \longleftrightarrow Na^+$ ion exchange waveguide splitter 1×2; $W_M = 8$ µm, $w = 1.2$ µm.

terference section and access waveguide and their propagation constants. Distribution profiles of heated waveguides are calculated on the basis of two-step nonlinear diffusing equation [9]. Table 7 shows the working characteristics (including the number of guided modes) for splitters obtained by $Ag^+ \longleftrightarrow Na^+$

T a b l e 7. Insertion losses for different times of heating.

Mode number	Time of heating (t_h/t_D)	L_{3dB} [μm]	Loss α [dB]
15	0	509	1.060
15	0.33	498	1.017
15	0.66	490	0.997
15	1	487	0.944
14	1.33	493	1.623

exchange process for MMI structures produced in preliminary diffusion process through the window of the width of 20 μm and then heated in the time $t_h = 1/3, 2/3$, 1, 4/3 of preliminary diffusion time t_D. Input and output waveguides are made in the same process (preliminary diffusion through the window of 1.2 μm). As shown by our calculations an increase of the time of heating within the limit $(0-1)t_D$ reduces insertion loss, decreasing to a certain degree the coupling length L_{3dB}. The process can be used for the correction of the geometry and working characteristics of splitters obtained in the preliminary diffusion. Subsequent increase of the heating time decreases the number of guided modes increasing inserion losses.
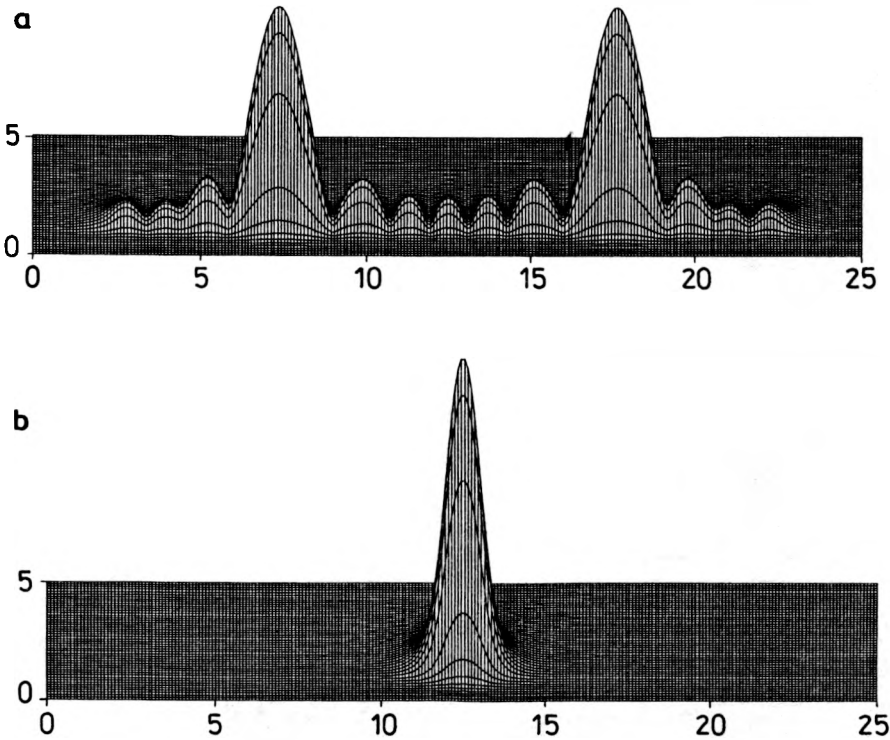

Fig. 8. Distribution of the field at the input (a) and output of interference section (b) obtained in the preliminary diffusion.
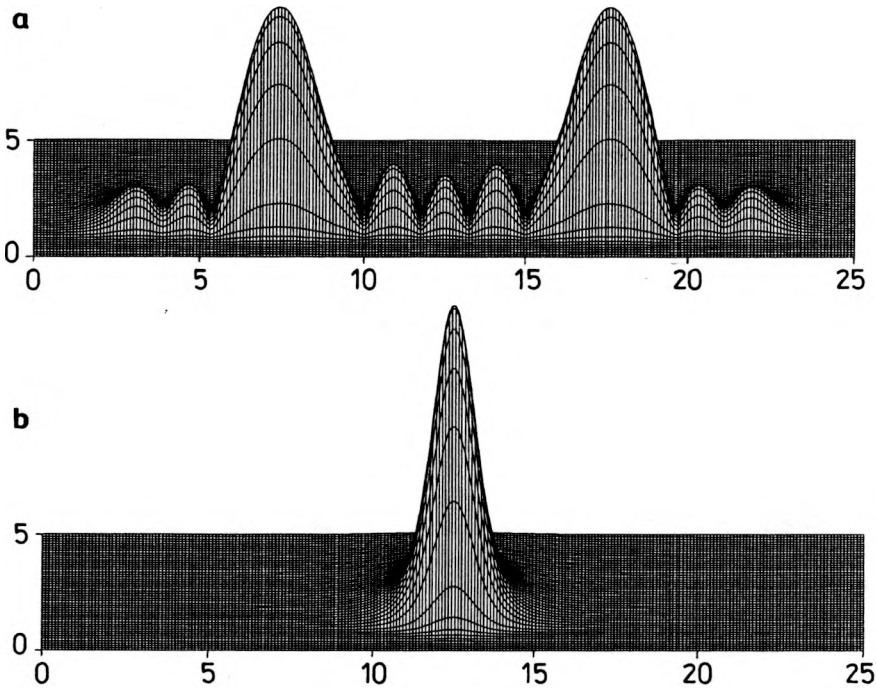
a

b

Fig. 9. Distribution of the field at the input (a) and output of interference section (b) after heating in the time $t_h = t_D$.

Figures 8 and 9 present, for comparison, field distributions at the output of interference sections and input field distributions for the waveguides obtained in preliminary diffusion process and after heating in the time $t_h = t_D$.

5. Mach–Zehnder interferometers

Systems of gradient MMI optical waveguide couplers and splitters can be used in Mach–Zehnder interferometer technology of different configurations. A diagram of the Mach–Zehnder interferometer structure examined is presented in Fig. 10. It consists of a pair of symmetrical MMI structures working as a 1×2 wave-
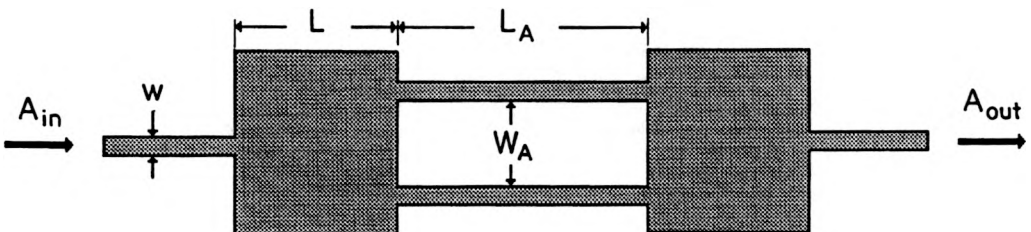

Fig. 10. Diagram of Mach–Zehnder interferometer structure under examination.

guide splitter and coupler, respectively, connected through the interferometer arms of the length L_A and separation distance w_A.

Insertion loss α [dB] in Mach–Zehnder interferometer, taking into consideration the input field imaging inaccuracy in both interference sections described by the equation

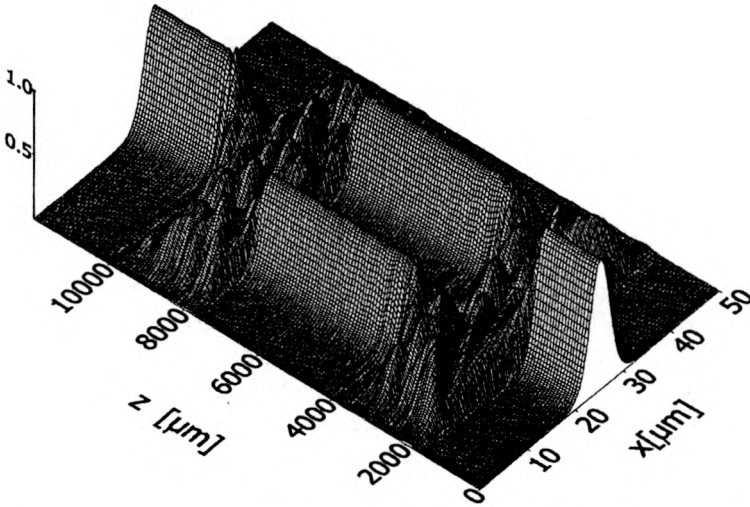$$\alpha = -20 \log \frac{A_{\text{out}}}{A_{\text{in}}}. \tag{5}$$

Fig. 11. Mach–Zehnder interferometer made in $K^+ \longleftrightarrow Na^+$ ion exchange; $W_M = 40$ μm, $w = 5$ μm.
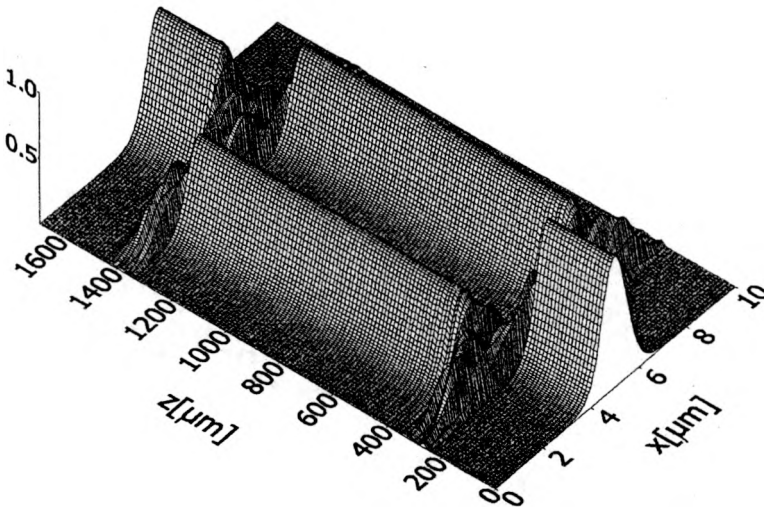

Fig. 12. Mach–Zehnder interferometer made in $Ag^+ \longleftrightarrow Na^+$ ion exchange; $W_M = 8$ μm, $w = 1.2$ μm.

A numerical simulation of the operation of Mach–Zehnder interferometer made in $K^+ \longleftrightarrow Na^+$ ion exchange for optimum section width W_M of 40 μm, excited with access waveguide field of the window width $w = 5$ μm is shown in Fig. 11. The length L_A and separation distance of interferometer arms w_A amout to 4000 μm and 20 μm, respectively. The splitting and coupling of the access field is carried out in MMI section of the length of 2120 μm. Insertion loss is 1.033 dB, including coupling losses at the output and input of MMI and inaccuracy of imaging of the input field.

Application of $Ag^+ \longleftrightarrow Na^+$ ion exchange makes it possible to decrease the total dimension of interferometer. Figure 12 shows the field evolution in Mach–Zehnder interferometer made in $Ag^+ \longleftrightarrow Na^+$ ion exchange for optimum geometry $W_M = 8$ μm and $w = 1.2$ μm. The length of interferometer arms L_A is assumed to be 1000 μm and their separation w_A amounts to 4 μm. The splitting and coupling length of MMI section is equal to 181 μm. Insertion loss is almost the same as for $K^+ \longleftrightarrow Na^+$ ion exchange and amounts to 1.06 dB.

6. Summary

In the paper, numerical studies of gradient index optical splitters made using a MMI technology by BPM method have been presented. The MMI structures produced in $K^+ \longleftrightarrow Na^+$ and $Ag^+ \longleftrightarrow Na^+$ ion exchange processes have been compared. Our investigation concerns the MMI structure geometry and technological process optimizations. We have concentrated on the influence of the window width of the input waveguides and multimode section and the heating of waveguide obtained in preliminary diffusion process. Based on the results of our study we were able to draw the following conclusions:

— Window width of single-mode input and output waveguides should be as big as to ensure good guiding conditions — preferably near the cut-off point of the first of higher order mode.

— Insertion losses increase together with MMI structure width in $K^+ \longleftrightarrow Na^+$ and $Ag^+ \longleftrightarrow Na^+$ ion exchange processes. MMI sections of both exchange processes guiding similar mode number show comparable insertion losses.

— Increase of the time of heating in the limit $(0-1)$ time of preliminary diffusion reduces insertion loss, decreasing to a certain degree the coupling length L_{3dB}. The heating can be used to correct the geometry and working characteristics of splitters obtained in the preliminary diffusion.

Making use of the self-imaging effects of input field in gradient ion exchanged MMI structures, optical waveguide splitters, couplers and Mach–Zehnder interferometers can be produced having very good optical parameters, where the branching of input field is realized over a very small area of a few hundred micrometers.

References

[1] SOLDANO L. B., PENNINGS E. C. M., J. Lightwave Technol. **13** (1995), 615.

[2] RAJARAN M., RAHMAN B. M. A., WONGCHAROEN T., BUAH P. A., GRATTAN K. T. V., Proc. SPIE **2954** (1996) 50.

[3] WIENERT C. M., AGRAWAL N., IEEE Photonic Technol. Lett. **7** (1995), 529.

[4] BŁAHUT M., Opt. Appl. **29** (1999), 111.

[5] YEVICK D., ROLLAND C., HEMMANSSON B., Electron. Lett. **25** (1989), 1254.

[6] PRESS W. H., FLANNERY B. P., VETTERLING W. T., *Numerical Recipes: The Art of Scientific Computing*, Cambridge Univ., New York 1986.

[7] HADLEY G. R., Opt. Lett. **16** (1991), 624.

[8] BŁAHUT M., OPILSKI A., ROGOZIŃSKI R., Opt. Appl. **22** (1992), 161.

[9] OPILSKI A., ROGOZIŃSKI R., BŁAHUT M., GUT K., KARASIŃSKI P., OPILSKI Z., Opt. Eng. **36** (1997), 1625.